

3D FE Analysis of anchor channels and headed anchors under shear load close to the edge

P. Grosser, R. Eligehausen & J. Özbolt

Institute of Construction Materials, University of Stuttgart, Germany

ABSTRACT: In the present paper the results of a finite element study of anchor channels and single headed anchors close to the free edge loaded in shear perpendicular and parallel to the edge (concrete edge failure) are discussed. For single headed anchors experimental tests and numerical simulations have been performed to investigate the load bearing behavior under arbitrary shear load (Hofmann 2005, Grosser 2008). In case of a headed anchor subjected to a shear force parallel to the free edge the failure is initiated by a splitting force acting perpendicular to the edge. It is a fraction of the applied shear load. In order to account for the fact that a higher shear load acting parallel to the edge is required to cause concrete edge failure compared to a shear load acting perpendicular to the edge in the draft fib Design Guide (fib (2009)) the calculated concrete edge capacity valid for a shear load perpendicular to the edge is multiplied by an increase factor. This factor primarily depends on the pressure in front of the anchor. For anchor channels arranged perpendicular to the edge and subjected to a shear load applied parallel to the edge limited experimental investigations performed by Roik (2009) indicate that the increase factor is higher compared to headed anchors. The non-linear finite element program MASA was used to study the load bearing behavior of headed anchors and anchor channels loaded perpendicular and parallel to the edge. It was verified that for anchor channels the ratio failure load (shear load parallel to the edge) to failure load (shear load perpendicular to the edge) is larger than for headed anchors. This is explained by the significantly lower pressure on the concrete in front of the channel compared to headed anchors.

1 INTRODUCTION

A single headed anchor close to the edge loaded in shear parallel to the edge may fail by a concrete edge breakout. A typical breakout pattern is shown in Figure 1a. The breakout pattern is similar to an anchor loaded by a shear load perpendicular to the edge. Only in front of the anchor the local spalling is more pronounced.

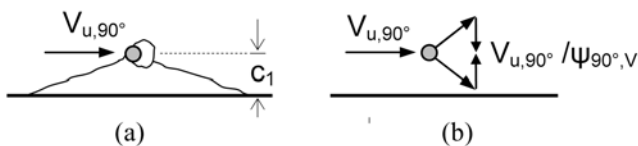


Figure 1. (a) Typical breakout pattern for a single anchor loaded parallel to the edge (b) Splitting forces caused by a shear load parallel to the edge.

The failure is caused by the splitting force in front of the anchor (Fig. 1b) which is a fraction of the applied shear force. In Figure 2 the distribution of stresses in front of the anchor caused by the shear force is shown. The ratio splitting force to shear force depends on the pressure in front of the anchor related to the concrete compressive strength.

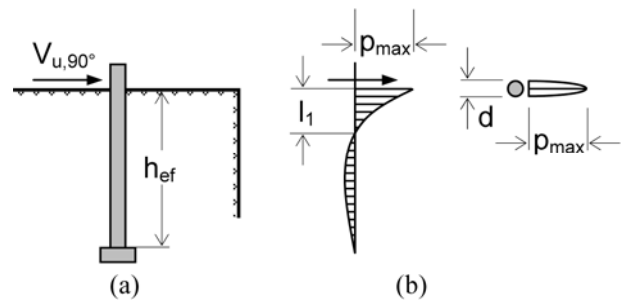


Figure 2. (a) Single anchor bolt subjected to a shear load (b) Stress distribution (schematic).

Therefore the concrete edge failure load for a shear force acting parallel to the edge may be calculated according to Equation (1).

$$V_{u,90^\circ} = V_{u,0^\circ} \left/ \left(v_1 \cdot \left(\frac{p}{f_{cc}} \right)^x \right) \right. \quad (1)$$

In Equation (1) p denotes the pressure in front of the anchor, $V_{u,0^\circ}$ the concrete edge failure load when loading the anchor perpendicular to the edge and $V_{u,90^\circ}$ the concrete edge failure load when loading the anchor parallel to the edge.

Hofmann (2005) assumes a linear relationship between the splitting force and the pressure in front of the anchor in the direction of loading ($x = 1$). The pressure p is defined as the quotient of the acting shear load and the area of the pressure zone in front of the anchor. This area is assumed to be $A = d^2$ ($d =$ bolt diameter). Based on the evaluation of test results, the factor ν_I is taken as 0.06. Rearranging Equation (1) leads to the increase factor according to Equation (2a).

$$V_{u,90^\circ} = \psi_{90^\circ,V} \cdot V_{u,0} \quad (2)$$

$$\text{with: } \psi_{90^\circ,V} = 4.0 \cdot \sqrt{\frac{d^2 \cdot f_{cc}}{V_{u,0}}} \quad (2a)$$

Experimental and numerical investigations have shown that the $\psi_{90^\circ,V}$ -factor decrease with increasing edge distance and decreasing anchor diameter. This is shown in Figure 3. Instead of calculating the $\psi_{90^\circ,V}$ -factor according to Equation (2a) the value $\psi_{90^\circ,V}$ can be taken as a constant with the lowest value obtained in tests. This simplification was adopted in the draft fib Design Guide (fib (2009)) and $\psi_{90^\circ,V} = 1.5$ was chosen.

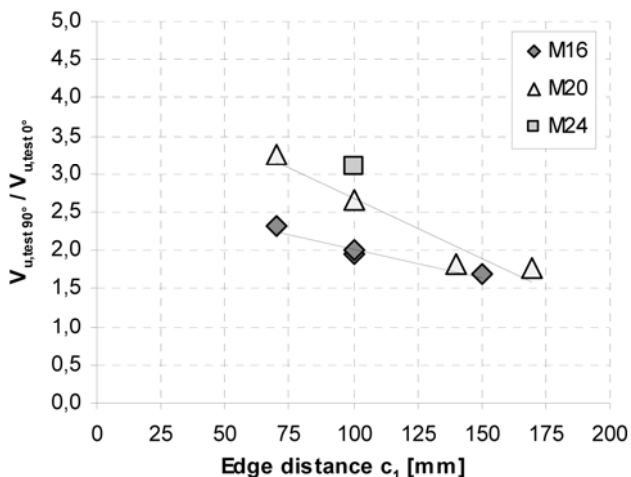


Figure 3. Influence of the edge distance and the anchor diameter on the increase factor $\psi_{90^\circ,V}$. Results of tests with single anchors loaded parallel and perpendicular to the edge.

When loading anchor channels by a shear load, the load is mainly transferred into the concrete by the channel profile. The anchors are mainly needed to take up the tension forces generated by the eccentricity between acting shear load and resulting compression force in the concrete (Potthoff (2008)). When loading an anchor channel with two anchors by a shear load, which is applied over one anchor (see Fig. 4a), only a part of the channel profile is activated. In case of an anchor channel subjected to a shear load parallel to the edge only limited experimental investigations exist. Therefore, in the draft fib Design Guide (fib (2009)) a factor $\psi_{90^\circ,V} = 1.5$ is assumed for the case of an anchor channel arranged

perpendicular to the edge and loaded in shear parallel to the edge, which acts over the front anchor (see Fig. 4b). To investigate if this simplification is justified and to understand the load bearing behavior of anchor channels loaded in shear parallel to the edge, numerical simulations were performed using the three-dimensional finite element program MASA.

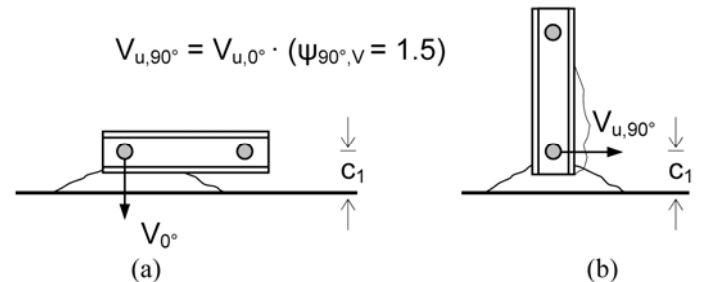


Figure 4. (a) Anchor channel arranged parallel to the free edge and loaded perpendicular to the edge (b) Anchor channel arranged perpendicular to the free edge and loaded parallel to the edge.

2 FINITE ELEMENT CODE MASA

2.1 General

The finite element program MASA has been developed at the Institute of Construction Materials, University of Stuttgart, and can be used to perform two and three-dimensional non-linear analysis for structures made of quasi-brittle materials such as concrete. Numerous simulations have shown that the finite element code MASA is capable to realistically represent the load bearing behavior of anchorages subjected to a shear load close to the edge.

2.2 Constitutive law – Microplane model

The FE code MASA used in the present study is based on the microplane model (Ožbolt et al. 2001) and a smeared crack approach. In the microplane model the material properties are characterized separately on planes of various orientations at a finite element integration point. On these microplanes there are only a few uniaxial stress and strain components and no tensorial invariance requirements need to be considered. The constitutive properties are entirely characterized by relations between the stress and strain components on each microplane in normal and shear direction. It is assumed that the strain components on the microplanes are projections of the macroscopic strain tensor (kinematic constraint approach). Knowing the stress-strain relationship of all components, the macroscopic stiffness and the stress tensor are calculated from the actual strains on the microplanes by integrating the stress components on the microplanes over all directions. Therefore only uniaxial stress-strain relationships

are required for each microplane component and the macroscopic response is obtained automatically by integration over all microplanes. To ensure mesh independent results a so-called “localization limiter” is used. Two different methods are implemented in MASA. Either the crack band approach (Bažant & Oh 1983) or the non local integral approach (Ožbolt & Bažant 1996) can be employed. For the analysis presented in this paper the crack band approach was used. More details about the model can be found in Ožbolt et al. (2001).

The analysis is carried out displacement controlled. The displacement is applied incrementally in several steps. For the preparation of the model (pre-processing) and the evaluation of the numerical results (post-processing) the commercial program FEMAP (Version 8.1) is used.

3 NUMERICAL INVESTIGATIONS

3.1 Model details and discretization

The discretization of the concrete member is performed using four node solid finite elements. As shown in Figure 5 the concrete slab is modeled with a length of $\geq 6c_1$ (c_1 = edge distance) for headed anchors and anchor channels arranged perpendicular to the edge and $\geq 6c_1+s$ (s = anchor spacing) for anchor channels arranged parallel to the edge, a width of $\geq 4c_1$ for headed anchors and anchor channels arranged parallel to the edge and $\geq 4c_1+s$ for anchor channels arranged perpendicular to the edge and a height of $\geq 3c_1$.

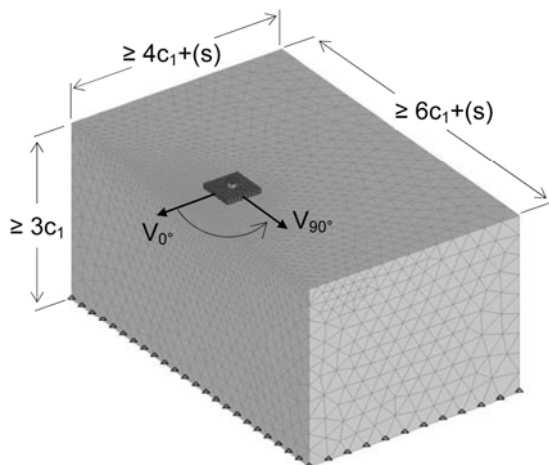
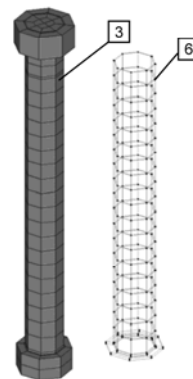
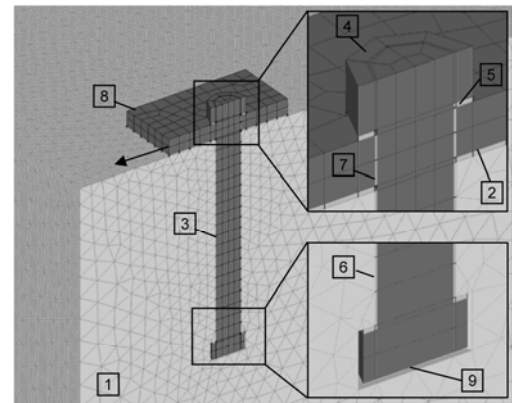


Figure 5. Geometry used in the finite element study.

The concrete properties are taken as: Cylinder compressive strength $f_c = 24$ MPa, cube compressive strength $f_{cc} = 28.5$ MPa, tensile strength $f_t = 1.9$ MPa, Young's modulus $E_C = 27,400$ MPa, Poisson's ratio $\nu_C = 0.18$ and fracture energy $G_F = 0.065$ N/mm. The behavior of steel is assumed to be linear elastic with Young's modulus $E_S = 210,000$ MPa and Poisson's ratio $\nu_S = 0.33$.

3.2 Headed anchors

In Figure 6 a section through the used model is shown in order to explain the several layers (see Table 1) and their functions.



1	Concrete
2	Teflon sheet + contact bars
3	Anchor bolt
4	Nut
5	Washer + contact bars
6	Contact layer + contact bars
7	Hole clearance + contact bars
8	Base plate
9	Air layer

Figure 6. Typical FE mesh of a headed anchor and contact elements.

To ensure a realistic load bearing behavior interface elements (thickness 0.5 mm) with contact bars which can take up only compressive stresses are introduced around the bolt and between the teflon sheet and concrete. A small gap around the head and at the bottom of the headed anchor is introduced to take into account that there is no load transmission at this surface (see Fig. 6). A teflon sheet is modeled between the concrete specimen and the steel plate to minimize friction between the concrete and the steel surface. Additionally a nut, washer and a clearance hole in the plate are modeled to consider realistically the stiffness of the connection between anchor bolt and base plate. The geometrical properties for all investigated cases are summarized in Table 2. All anchors are loaded perpendicular and parallel to the edge.

Table 2. Geometric properties.*

test	c_1	d_{anchor}	d_{head}	h_{ef}	α [-]**
A1	40	6	12	45	0°/90°
A2	75	10	20	94	0°/90°
A3	100	10	20	94	0°/90°
A4	100	16	32	130	0°/90°
A5	100	22	44	130	0°/90°
A6	150	16	32	179	0°/90°

* Dimensions in [mm]

** 0° = shear load towards the edge

90° = shear load parallel to the edge

The boundary conditions were defined as nodal load and constraints. A shear load parallel to the edge is applied to only one node to allow a hinged load application (see Fig. 6). For comparison the behavior for a shear loading acting perpendicular to the edge is investigated as well. All nodes at the bottom of the concrete member are supported in vertical direction to avoid tilting of the slab. In load direction only one line at the bottom of the front surface is supported. Additionally two further nodes in the third dimension are restraint due to the fact that the numerical model requires constraints in every direction.

3.3 Anchor channels

The model used for the numerical simulations of anchor channels is shown in Figure 7. Three different sizes of anchor channels (28/15, 50/30 and 72/48) are modeled. Anchor channels 50/30 and 72/48 are hot rolled profiles (type 1) and channel 28/15 is a cold rolled profile (type 2).

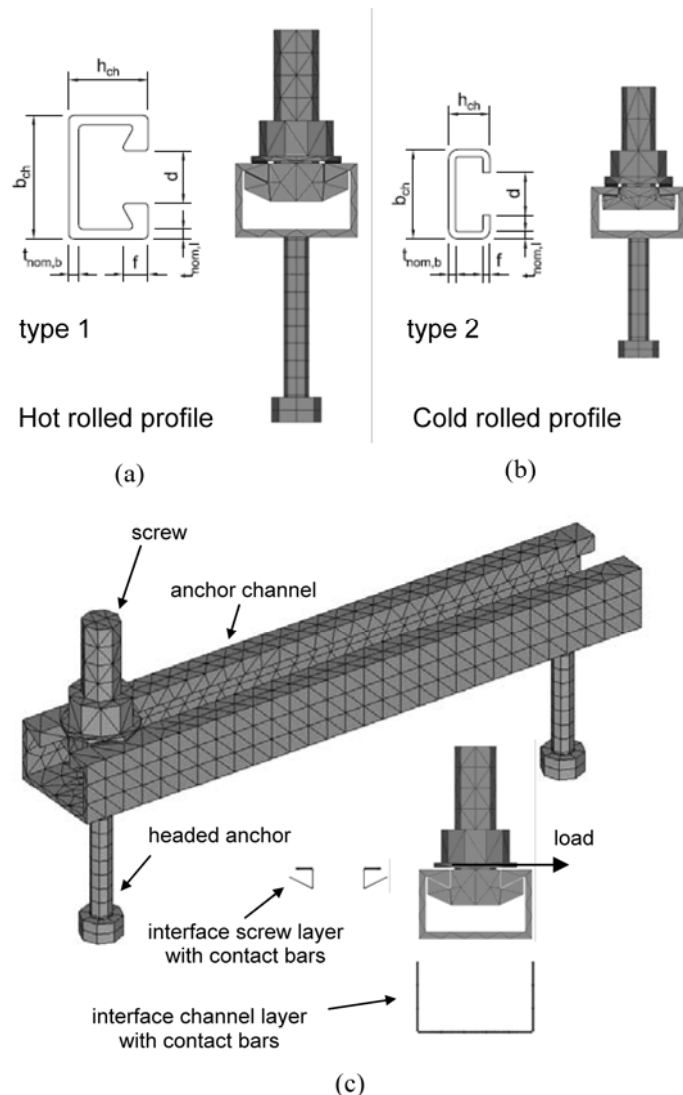


Figure 7. (a) Type 1 (hot rolled profile) (b) Type 2 (cold rolled profile) (c) Typical FE mesh of an anchor channel and contact elements.

When loading an anchor channel under shear the load is mainly transferred by compressive stresses in front of the channel profile and to a small part by the anchors. Therefore interface elements with contact bars which can only take up compressive stresses are modeled around the anchor channel to avoid the transmission of tensile stresses. Numerical investigations without this layer have shown that the failure loads are significantly overestimated. The anchors fixed to the channel are modeled according to chapter 3.2.

The geometrical properties of all investigated cases are summarized in Table 3. As for headed anchors, all anchor channels are loaded perpendicular and parallel to the edge. The boundary conditions were defined as described in chapter 3.2. The shear load is applied to only one node on the screw (see Fig. 7c).

Table 3. Geometric properties.

channel	type	d_{anchor}	d_{head}	c_1	s	h_{ef}	α [-]
28/15	2	6	12	40	200	45	0°/90°
50/30	1	10	20	75	250	94	0°/90°
50/30	1	10	20	100	250	94	0°/90°
72/48	1	16	32	150	400	179	0°/90°

4 ANALYSIS OF THE NUMERICAL INVESTIGATIONS AND COMPARISON WITH TEST DATA

4.1 Headed anchors

In both the experimental and the numerical investigations a characteristic concrete edge failure could be observed. A typical failure pattern is shown in Figure 8.

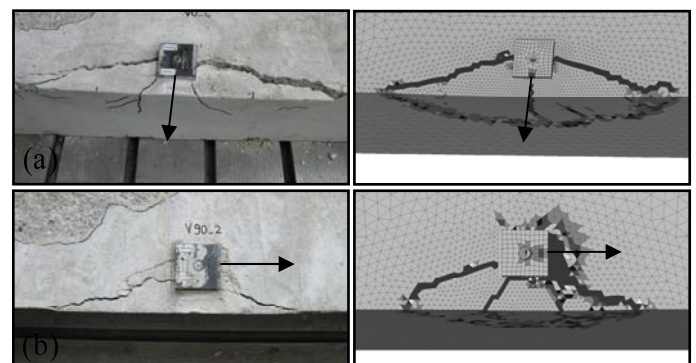


Figure 8. Post peak crack pattern, $c_1 = 100$ mm (edge distance), $h_{\text{ef}} = 130$ mm (embedment depth), load direction (a) perpendicular (b) parallel to the edge, left: test result, right: numerical investigation.

In Figure 9 the load-displacement curves observed in the experiments and the numerical simulations are compared. The agreement of the numerical obtained failure pattern and load-displacement behavior with the test observations is very good.

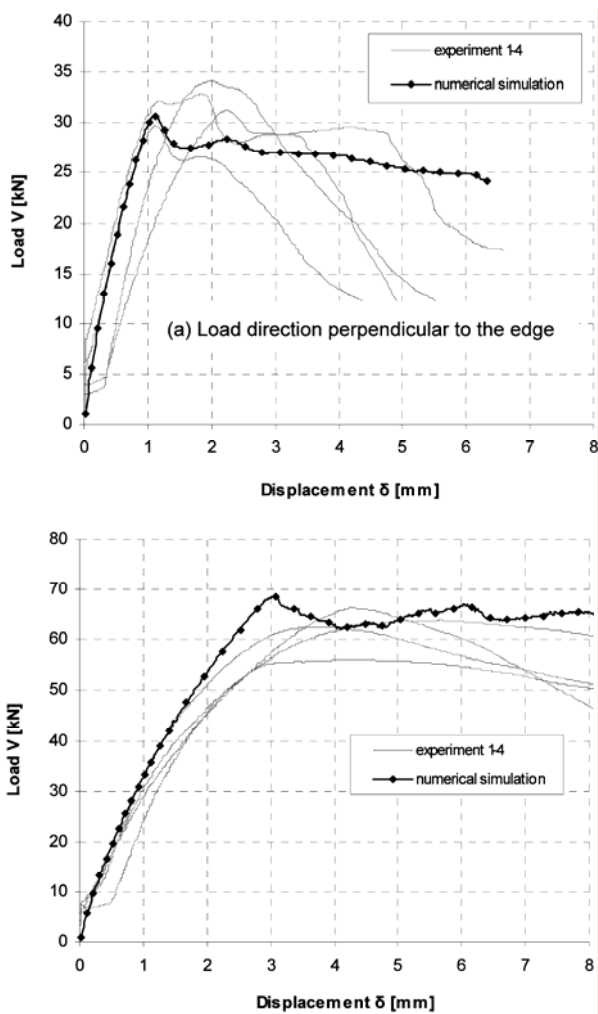


Figure 9. Load-displacement curves of headed anchors, $c_1 = 100$ mm (edge distance), $h_{ef} = 130$ mm (embedment depth), load direction (a) perpendicular (b) parallel to the edge.

A summary of the results of the simulated headed anchors is shown in Table 4. For comparison, in the same table the predictions for a single anchor loaded by a shear load perpendicular to the edge according to Equation (3) are shown. Equation (3) has been proposed by Hofmann (2005).

$$V_{u,c,0^\circ} = 3.0 \cdot d^\alpha \cdot h_f^\beta \cdot \sqrt{f_{cc}} \cdot c_1^{1.5} \quad (3)$$

with:

$$\alpha = 0.1 \cdot \left(\frac{h_{ef}}{c_1} \right)^{0.5} \quad \beta = 0.1 \cdot \left(\frac{d}{c_1} \right)^{0.2}$$

Table 4. Summary of the results.

Test	c_1	$V_{u,num,0^\circ}$	$V_{u,c,0^\circ}^{1)}$	$V_{u,num,0^\circ} / V_{u,c,0^\circ}$	$V_{u,num,90^\circ}$
A1	40	6.51	6.36	1.02	17.97
A2	75	19.07	18.24	1.05	49.77
A3	100	29.05	26.67	1.09	54.46
A4	100	30.69	30.79	1.00	69.32
A5	100	32.66	32.64	1.00	81.02
A6	150	56.96	55.49	1.03	102.6

Loads in [kN], Dimensions in [mm]

¹⁾ $V_{u,c,0^\circ}$ according to Equation (3)

The numerical results agree very well with the values calculated according to Equation (3).

4.2 Anchor channels

In the experimental investigations both concrete failure and steel failure could be observed due to the low steel strength of the screw and the anchor channel. In the numerical simulations the behavior of the steel is assumed to be linear elastic to avoid steel rupture. In Figure 10 and Figure 11 a typical concrete edge failure obtained in the experimental and numerical investigations is shown.

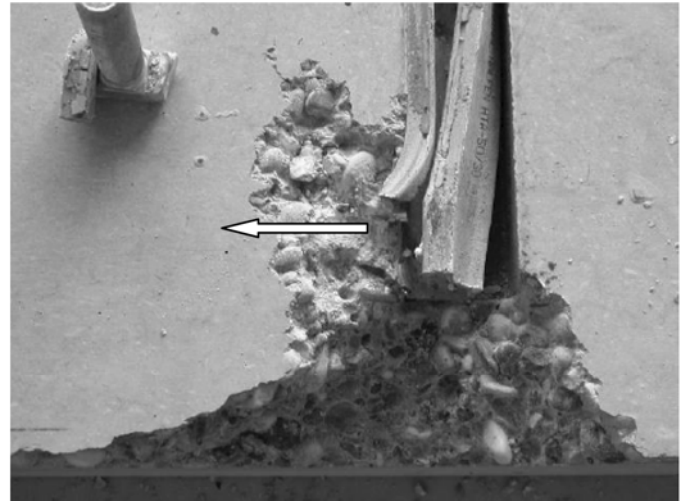


Figure 10. Post peak crack pattern, anchor channel 50/30, $c_1 = 100$ mm (edge distance), $s = 150$ mm (spacing), tests by Roik (2009).

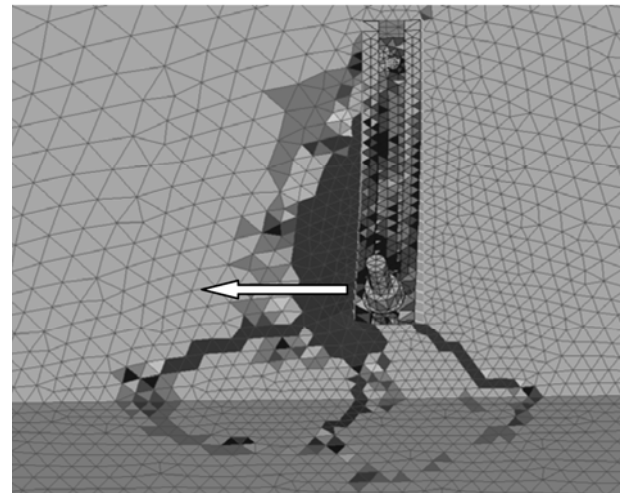


Figure 11. Numerically obtained post peak crack pattern, anchor channel 50/30, $c_1 = 100$ mm (edge distance), $s = 250$ mm (spacing).

Table 5 summarizes the numerical results of the anchor channels loaded perpendicular and parallel to the edge. For comparison, the predictions for an anchor channel loaded by a shear load perpendicular to the edge according to Equation (4) are shown. Equation (4) has been proposed by Potthoff (2008).

$$V_{u,c,0} = \alpha \cdot \sqrt{f_{cc}} \cdot c_1^{1.5} \quad (4)$$

α_p = channel profile factor

(5.0 for 28/15)(6.0 for 50/30)(7.0 for 72/48)

4.3 Numerically obtained $\psi_{90^\circ,V}$ -factors

In Figure 12 the obtained factors $\psi_{90^\circ,V}$ for the simulated headed anchors and anchor channels are plotted as a function of the edge distance. They decrease with increasing edge distance. Furthermore for headed anchors with a constant edge distance they increase with increasing anchor diameter. These findings agree with the results shown in Figure 3. The $\psi_{90^\circ,V}$ -factors valid for anchor channels are significantly higher than for headed anchors. In Table 6 the factors $\psi_{90^\circ,V}$ for anchor channels and headed anchors are compared with each other. The factors $\psi_{90^\circ,V}$ for anchor channels are between about 4.5 ($c_1 = 40$ mm) and 3.0 ($c_1 > 100$ mm) and for headed anchors between about 2.7 ($c_1 = 40$ mm) and 1.7 ($c_1 = 150$ mm). The factors $\psi_{90^\circ,V}$ for anchor channels are valid for the allowable minimum edge distance of the different channel sizes. When for a given channel size the edge distance is increased, the factor $\psi_{90^\circ,V}$ will decrease. However in the tests by Roik (2009) with anchor channels with minimum edge distance, partly failure of the channel lips with breaking of the special screw out of the channel profile occurred. Therefore when the edge distance is increased significantly, steel failure and no concrete edge failure will occur.

Table 6. Comparison of the results.

anchor channel	headed anchor	c_1 [mm]	d [mm]	$\Psi_{90^\circ,V}$ channel	$\Psi_{90^\circ,V}$ anchor	$\Psi_{90^\circ,V,channel} / \Psi_{90^\circ,V,anchor}$
28/15	A1	40	6	4.53	2.76	1.64
50/30	A2	75	10	3.55	2.61	1.36
50/30	A4	100	10	3.09	2.26	1.37
72/48	A6	150	16	3.18	1.80	1.77

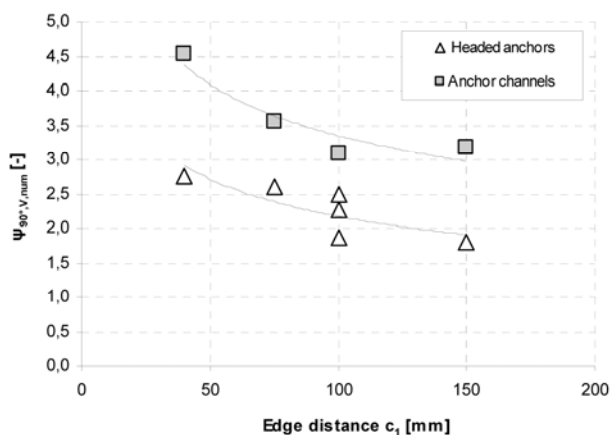


Figure 12. Increase factor $\psi_{90^\circ,V}$ obtained in numerical simulations versus edge distance.

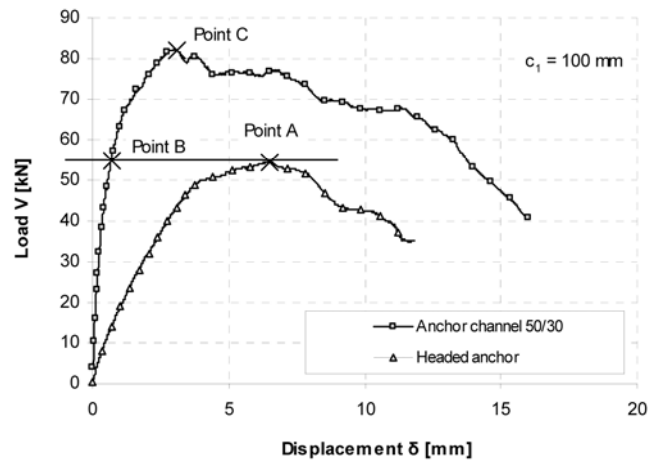


Figure 13. Load-displacement curves of anchor channel 50/30 ($d = 10$ mm) and headed anchor ($d = 10$ mm, $h_{ef} = 94$ mm) for an edge distance $c_1 = 100$ mm.

To investigate the reason for the higher factors $\psi_{90^\circ,V}$ for anchor channels, the stress distribution in front of a headed anchor and a channel profile with the same edge distance as the anchor is compared for the same load level (peak load of headed anchor, see Fig. 13, Point A and B). Furthermore the compressive stresses at peak load of the anchor channel are evaluated (Point C in Fig. 13). The diameter of the anchor fixed to the channel profile agrees with the diameter of the tested headed anchor. In Figure 14 the compressive stresses in the concrete in the vicinity of the headed anchor with a diameter $d = 10$ mm and an embedment depth $h_{ef} = 94$ mm are shown at ultimate load. In Figure 15a the distribution of the compressive stresses in front of the headed anchor along the upper part of the embedment depth are plotted. Figure 15b shows the distribution of the compressive stresses along three cross sections, which are shown in Figure 14. Figure 15 is valid for peak load of the headed anchor.

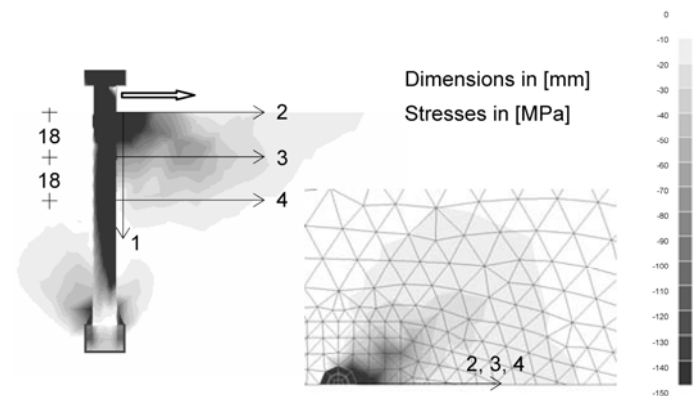


Figure 14. Compressive stresses at ultimate load.

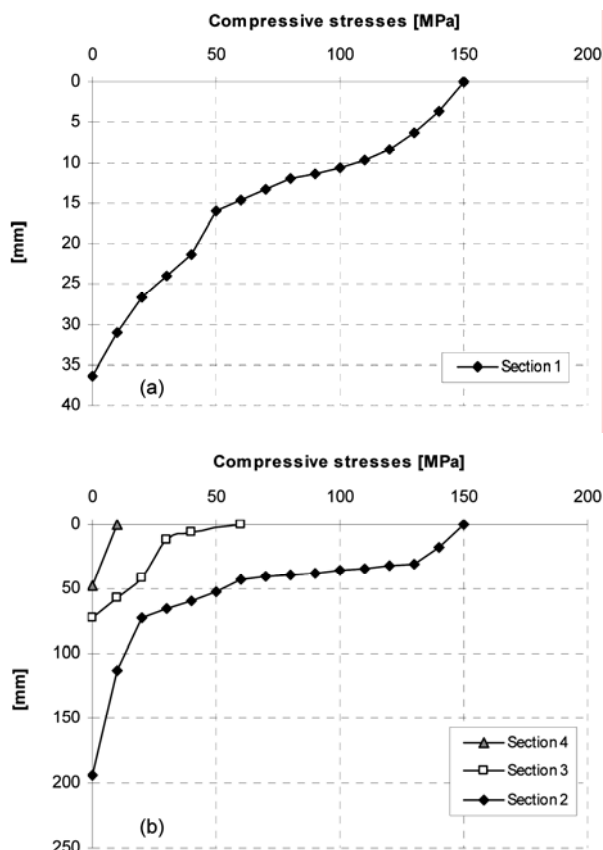


Figure 15. Compressive stresses at peak load (a) in front of the headed anchor along the embedment depth (Section 1) (b) in bolt axis in sections 2 to 4 (location of sections see Fig. 14).

The maximum pressure $p_{max} = 150$ MPa is approximately $5 \cdot f_{cc}$. The depth of the compressed zone is about $3.5 \cdot d$. With increasing distance to the anchor bolt, the compressive stresses decrease rapidly.

In Figure 16 the compressive stresses in the vicinity of the anchor channel 50/30 are shown. In Figure 17a the distribution of the compressive stresses in front of the anchor channel as a function of the distance from the concrete surface is plotted. Figure 17b shows the compressive stresses in cross section 2 and 3. Section 2 is located at the concrete surface and section 3 at the lower end of the channel profile (see Fig. 16). Parameter is the applied shear load (equal with peak load of headed anchor and peak load of anchor channel).

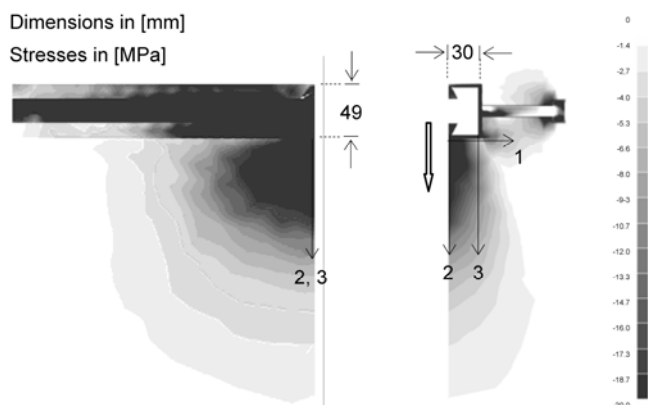


Figure 16. Compressive stresses in the vicinity of anchor channel, load at Point B of load-displacement curve.

The maximum pressure in front of the channel profile is much lower than for a headed anchor. At a shear load equal to the peak load of the headed anchor it amounts to about 20 MPa ($\sim 2/3 \cdot f_{cc}$) and at peak load of the anchor channel the maximum pressure $p_{max} = 28$ MPa is approximately f_{cc} . Below the channel profile, the compressive stresses increase due to the load transfer by the anchors fixed to the channel. The compressive stresses decrease towards the concrete surface because of spalling of the concrete in front of the channel. As with headed anchors, with increasing distance from the channel the compressive stresses decrease rapidly.

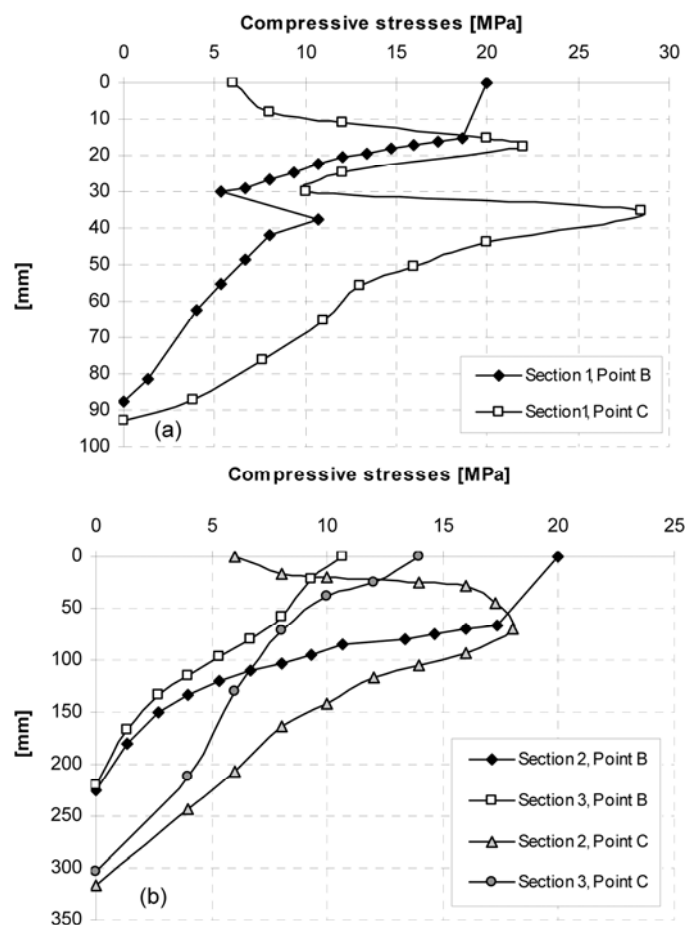


Figure 17. Compressive stresses for load B (peak load of headed anchor) and load C (peak load of anchor channel) (a) in front of the anchor channel as a function of the distance from the concrete surface (Section 1) (b) in Section 2 (concrete surface) and Section 3 (lower end of channel profile) as a function of the distance from the channel.

According to Equation (2) the ratio $\psi_{90^\circ, V} = V_{u,90^\circ} / V_{u,0^\circ}$ decreases with increasing pressure. The pressure in front of headed anchors averaged over about d^2 is about four times higher than the values valid for anchor channels. This explains the higher factors $\psi_{90^\circ, V}$ for anchor channels compared to headed anchors with the same edge distance.

5 SUMMARY AND CONCLUSIONS

In the present study the behavior of headed anchors as well as anchor channels close to an edge under shear load is numerically investigated. Two load cases are studied (i) shear load is applied perpendicular to the free edge (ii) shear load is applied parallel to the free edge. The numerical results are compared with limited test data and current design recommendations. It is shown that the numerical model is able to represent realistically the load-bearing behavior of anchorages subjected to a shear load close to the edge. The aim of the study is to evaluate the relationship between the failure loads when the shear load is applied parallel and perpendicular to the edge (factor $\psi_{90^\circ, V}$) (see Equation (2)). Therefore the $\psi_{90^\circ, V}$ -factors obtained in the numerical simulations of anchor channels and headed anchors are compared.

Based on the results of the numerical investigation, the following can be concluded: a) The factors $\psi_{90^\circ, V} = V_{u,90^\circ}/V_{u,0^\circ}$ of anchor channels are about 1.4 to 1.8 (on average 1.5) times larger than for headed anchors. This can be explained as follows: In case of a shear load parallel to the edge the failure is caused by splitting forces. These splitting forces decrease with decreasing pressure in front of the anchor or channel profile and for anchor channels the pressure in front of the channel profile is much lower than for headed anchors. b) It is proposed to calculate the mean concrete edge failure load of anchor channels arranged perpendicular to the edge and loaded by a shear load parallel to the edge by Equation (2) with $V_{u,0^\circ}$ according to Equation (4) and $\psi_{90^\circ, V} = 2.5$. To improve this design recommendation and extend its validity to other applications further theoretical, experimental and numerical studies are recommended.

ACKNOWLEDGEMENT

The authors wish to express special thanks to the company Halfen for the financial and technical support and special thanks to DKG (Deutsche Kahneisen Gesellschaft) for the financial support.

REFERENCES

- Bažant, Z. P.; Oh B. H. 1983. Crack band theory for fracture of concrete. *Materials and Structures*, 93 (16): 155-77.
- Grosser, P. 2008. *Fastenings under shear loading parallel to the edge*. Test Report No. E08/02-G07100/03, IWB, Universität Stuttgart, not published.
- Hofmann, J. 2005. *Tragverhalten und Bemessung von Befestigungen unter beliebiger Querbelastung in ungerissenem Beton (Behaviour and design of anchorages under arbitrary shear load direction in non-cracked concrete)*. Dissertation, IWB, Universität Stuttgart (in German).
- fib 2009. International Federation for Structural Concrete (fib). *Design of anchorages to concrete structures*. Final draft. Publication is expected in 2010
- Ožbolt, J., Bažant, Z. P. 1996. Numerical smeared fracture analysis: Nonlocal microcrack interaction approach. *International Journal for Numerical Methods in Engineering*. 39 (4): pp. 635-661
- Ožbolt, J.; Li, Y; Kožar 2001. Microplane model for concrete with relaxed kinematic constraint. *International Journal of Solid and Structures*. 38 (16): pp. 2683-2711.
- Potthoff, M. 2008. *Tragverhalten und Bemessung von Ankerschienen unter Querbelastung (Behaviour and design of anchor channels under shear load)*. Dissertation, IWB, Universität Stuttgart (in German).
- Roik, M. 2009. *Tastversuche zum Tragverhalten von senkrecht zum Rand eingebauten Ankerschienen, belastet durch Querzug parallel zum Rand (Preliminary tests to anchor channels arranged perpendicular to the edge and loaded by a shear load parallel to the edge)*. Langenfeld: Halfen GmbH, not published (in German).